Momentum Loss in Proton-Nucleus and Nucleus-Nucleus Collisions

Ferdous Khan and
Lawrence W. Townsend

Momentum Loss in Proton-Nucleus and Nucleus-Nucleus Collisions

Ferdous Khan
Old Dominion University
Norfolk, Virginia

Lawrence W. Townsend
Langley Research Center
Hampton, Virginia

Abstract

An optical model description, based on multiple scattering theory, of longitudinal momentum loss in proton-nucleus and nucleus-nucleus collisions is presented. The crucial role of the imaginary component of the nucleon-nucleon transition matrix in accounting for longitudinal momentum transfer is demonstrated. Results obtained with this model are compared with Intranuclear Cascade (INC) calculations, as well as with predictions from Vlasov-Uehling-Uhlenbeck (VUU) and quantum molecular dynamics (QMD) simulations. Comparisons are also made with experimental data where available. These comparisons indicate that the present model is adequate to account for longitudinal momentum transfer in both proton-nucleus and nucleus-nucleus collisions over a wide range of energies.

1. Introduction

Propagation of a particle in the nuclear medium is characterized by its mean free path (refs. 1, 2, and 3). At incident energies of 50–150 MeV, the experimental mean free path for protons is known (refs. 4, 5, and 6) to be approximately 5–6 fm. Theoretical calculations yield a value of similar magnitude only when Pauli blocking effects and the nonlocality of the optical potential are taken into account. These non-local effects can be satisfactorily accounted for only in the limit, where the imaginary part of the optical potential is small and all results can be expanded to first order in the imaginary potential (ref. 2).

At high energies, however, the imaginary part of the optical potential is not small. In addition, the scattering cross section is extremely forward peaked. Thus, the concept of mean free path loses much of its significance as an indicator of how energy and momentum are exchanged. Alternate concepts, such as momentum degradation (or decay) length, have been introduced (ref. 7) in order to explore the inelasticities in nucleon-nucleon (NN) collisions at relativistic energies and their effects on nuclear stopping power. In nucleus-nucleus collisions, the first attempt to understand momentum degradation was based on a shock wave picture (ref. 7) where the nuclei were treated as colliding drops of "nuclear fluid" that formed a shock front where they met. The momentum degradation length λ' in this approach is defined in terms of the conventional mean free path $\lambda = (\rho_o \sigma_{NN})^{-1}$ as

$$\frac{\lambda'}{\lambda} = \frac{P_{\mathrm{CM}}}{\left\langle q_\| \right\rangle} \qquad (1)$$

where ρ_o is the nuclear number density, σ_{NN} is the free nucleon-nucleon cross section, P_{CM} is the NN center-of-mass momentum, and $\left\langle q_\| \right\rangle$ is the mean longitudinal momentum transfer per collision. These authors found that in general λ' is an increasing function of P_{CM} (fig. 1 of ref. 7). In particular, for bombarding energies from the pion production threshold up to $600A$ MeV, λ' remains approximately constant because of increased longitudinal momentum transfer and decreased elastic and quasi-elastic scatterings. Above $600A$ MeV, both P_{CM} and $\left\langle q_\| \right\rangle$ increase, but because they are nearly equal, λ' increases rather slowly.

Further attempts to understand nuclear stopping power at high energies have replaced the shock wave picture with a two-fluid model (ref. 8), coupled only by a frictional drag. This model successfully demonstrated that high baryon density can be achieved during mutual interpenetration of projectile and target nuclei without shock formation. The concept of momentum degradation length, however, has survived the above transformation in thinking about the nuclear stopping power. Anishetty et al. (ref. 9) examined the experimental data on pp (proton-proton) scattering and extracted information about proton stopping distance in high-energy collisions. Busza and Goldhaber (ref. 10) examined the proton-nucleus collision data and concluded that the mean rapidity loss suffered by a high-energy proton is $\approx -2.4 \pm 0.2$ units, which corresponds to a momentum loss of ≈ 4–7 GeV/c by the projectile nucleon in its rest frame. This is significantly higher than the momentum loss suffered by a proton in pp collisions (≈ 0.75–1.5 GeV/c) (refs. 9, 11, and 12). The sequential scattering models (SSM) were introduced (refs. 13–17) in order to explain the significantly

higher momentum loss in proton-nucleus collisions when compared with pp collisions. Csernai and Kapusta (ref. 17) defined the momentum degradation length in proton-nucleus collisions as

$$\Lambda_p = (\rho_o \sigma_{NN} I)^{-1} \qquad (2)$$

where I, called the inelasticity coefficient, plays essentially the same role as $\left\langle p_\parallel \right\rangle \big/ P_{\mathrm{CM}}$ in equation (1). This is not unexpected, since the mean longitudinal momentum transfer $\left\langle p_\parallel \right\rangle$ in NN collisions is intimately related to the degree of inelasticity in such collisions. A reasonable estimate (ref. 17) for Λ_p is

$$\Lambda_p = \left(\frac{1}{P_z} \frac{dP_z}{dz} \right)^{-1} \approx 5\text{--}6 \text{ fm} \qquad (3)$$

where P_z is the laboratory proton momentum. Note that not all versions of the SSM agree on this value of Λ_p, since they differ in their choices for the inelasticity coefficient I. The essence of these models can be illustrated by recalling that as an incident proton traverses a target, it loses some fraction of its momentum in each collision. Assuming a Poisson distribution where the mean number of collisions is characterized by $\overline{N}(z) = \rho_o \sigma_{NN} z$ (where z is the depth in femtometers), one may write for P_z

$$P_z = P_o e^{-\overline{N}} \sum_{N=0}^{\infty} \left(\frac{\overline{N}^N}{N!} \right) (1 - I)^N = P_o e^{-I\overline{N}} \quad (4)$$

Hence equation (2) follows.

In this regard, it is instructive to note that the rapidity loss distribution extracted (refs. 9–12) from pp collisions is Gaussian with a median rapidity loss shift of ≈ -0.7 and an average shift of ≈ -1 unit. In the rest frame of the incident proton, this translates into a root-mean-square momentum loss of $\approx 0.75 \text{ GeV}/c$ (1.5 GeV/c if a variable proton to baryon ratio is taken into account). It has been noted (ref. 10) that the momentum loss suffered by the proton in proton-nucleus collisions is roughly what it suffers in pp collisions times the number of inelastic collisions it is expected to undergo as it traverses the nuclear target.

Although the above models describe rapidity loss of high-energy (≥ 100 GeV) protons rather satisfactorily, it is not obvious which model will apply in the low- and intermediate-energy (10A MeV–several A GeV) domains. It is in the low- and intermediate-energy regimes that we focus our present attention.

The earliest evidence of energy and momentum loss in *relativistic* heavy ion (nucleus-nucleus) collisions in the few GeV domain comes from the observed "momentum downshifts" of projectile fragments in the pioneering experiments on relativistic heavy ion fragmentation using carbon and oxygen beams (refs. 18 and 19). In the projectile rest system, these momentum downshifts are small (typically tens of MeV/c). For charge-exchange channels, the measured momentum downshifts were larger (≈ 100 MeV/c). Gerbier et al. (ref. 20) reported a very large momentum downshift measurement of nearly 6 GeV/c for charge-pickup reactions of 900A MeV gold transforming into mercury in collisions with an aluminum target. This large downshift, however, has not been reproduced in subsequent experiments (ref. 21) where only small energy losses were measured (≈ 3–5A MeV). Recently, Tull (ref. 22) measured the momentum losses of projectile fragments for a 1.65A-GeV argon beam colliding with both carbon and potassium chloride targets. Reference 23 contains further information on momentum loss in heavy ion experiments. Experimental literature on stopping and compression in low-energy nucleus-nucleus collisions ($\leq 2A$ GeV) can be found in reference 24. Theoretical attempts to explain nuclear stopping in this energy domain can also be found in the latter reference.

The impetus for understanding momentum loss in proton-nucleus, as well as nucleus-nucleus, collisions within the multiple scattering theory framework of the present work was the desire to describe and predict fragment momentum distributions in low and intermediate energy ($\approx 10A$ MeV to a few GeV) heavy ion collisions. The salient feature of this model is the association of the gradient of the imaginary component of the NN transition matrix (folded with nuclear densities of the projectile-target system) with beam momentum loss (refs. 25 and 26). The real part of the transition matrix (folded with the nuclear densities) was previously shown to describe transverse momentum transfer (refs. 25 and 27).

The outline of the paper is as follows. In section 2, the expression for dynamical momentum loss is introduced, and the analogy with the sequential scattering models is pointed out for the proton-nucleus case. In section 3, results of beam momentum loss are presented for 85A-MeV ^{12}C-induced reactions on targets ranging from ^{12}C through ^{197}Au. The impact parameter dependence of momentum loss for the reaction ^{12}C(84A MeV) + ^{12}C is also presented and compared with simulations and model calculations, such as Vlasov-Uehling-Uhlenbeck (VUU), Boltzmann-Uehling-Uhlenbeck (BUU), Boltzmann-

Nordheim-Vlasov (BNV), and quantum molecular dynamics (QMD). Finally, in section 4 we conclude by summarizing the current status of model development and discuss future directions for experimental and theoretical research.

2. Momentum Degradation

In the optical model of momentum degradation, one describes momentum loss in composite targets within the multiple scattering theory framework (ref. 25) as a superposition of momentum losses by single NN collisions; that is, the latter is folded with the nuclear densities of the projectile-target system. For momentum loss in a single NN collision, the gradient of the imaginary part of the transition matrix is integrated from $-\infty$ to $+z$, where z is the depth (in fm), and the resulting expression is then folded with the nuclear density. Explicitly,

$$Q_{\parallel}(b,z) = A_P A_T \int d^3\xi_P \rho_P\left(\vec{\xi}_P\right) \int d^3\xi_T \rho_T\left(\vec{\xi}_T\right)$$
$$\times \left[\int_{-\infty}^{z} \nabla_{\xi P} \mathrm{Im}\, \tilde{t}\left(\overrightarrow{b+z'} + \overrightarrow{\xi_P - \xi_T}\right) \frac{dz'}{v}\right] \tag{5}$$

In the above expression, nuclear densities $\rho_i\,(i=P,T)$ are normalized to unity, $\xi_i\,(i=P,T)$ are the nuclear internal coordinates, A_i are the mass numbers of the colliding nuclei, $v = |\vec{v}|$ is the relative velocity in the nucleon-nucleon center-of-mass frame with kinetic energy $e = \frac{1}{2}\mu\vec{v}^2$, where μ is the reduced mass. The gradient (∇) is taken with respect to the projectile nucleus internal coordinates, and $\tilde{t}$ is the complex two-nucleon transition amplitude given by equation (15) of reference 25. The bracketed quantity in equation (5) is the momentum loss in a single NN encounter, $q_{\parallel}(\vec{r})$, with $r = |\vec{r}|$ the radial separation of the colliding pair. The imaginary part of the NN transition matrix is $\mathrm{Im}\,\tilde{t}$. Note that $Q_{\parallel}(\vec{b},z)$ depends on both $\vec{b}$ and z, although asymptotically ($z \to \infty$) it is only b (impact parameter) dependent.

Now consider the transition matrix at high energy

$$\tilde{t}(e,\vec{q}) \approx \frac{-\sqrt{em}}{4\pi}\sigma(e)\left[\alpha(e) + i\right]\exp\left(-\frac{1}{2}B(e)\vec{q}^2\right) \tag{6}$$

where e is the NN kinetic energy in its center of mass and m is the nucleon rest mass. The root-mean-square momentum transfer, obtained from the real part of equation (6), is related to the imaginary

component via an energy dependent ratio $\alpha(e)$, such that

$$\sqrt{\left\langle q_{\mathrm{Im}}^2\right\rangle} = \frac{\sqrt{\left\langle q_{\mathrm{Real}}^2\right\rangle}}{\alpha(e)} \tag{7a}$$

where $\alpha(e)$ is the ratio of real to the imaginary component of the NN forward scattering amplitude. The root-mean-square transverse momentum transfer is

$$\left\langle q_{\mathrm{Real}}^2\right\rangle = [B(e)]^{-1} = 0.3\text{--}0.4\,(\mathrm{GeV}/c)^2 \tag{7b}$$

so that from equation (7a), one arrives at the following estimate for longitudinal momentum transfer:

$$\sqrt{\left\langle q_{\mathrm{Im}}^2\right\rangle} \approx 0.75\text{--}2\,\mathrm{GeV}/c \tag{7c}$$

where an average of the experimental (absolute) values for $\alpha_{pp}(e)$ and $\alpha_{np}(e)$, which range between $\approx 0.2\text{--}0.4$ at high energy, was used. (The subscripts pp and np refer to proton-proton and neutron-proton, respectively.) The above estimate in equation (7c) is consistent with experimental momentum degradation data in pp collisions (refs. 9–12).

An important question is how the quantity $Q_{\parallel}$ in equation (5) is related, in the high-energy limit, to the predictions of the high-energy models such as the sequential scattering model (SSM). Recall that while $Q_{\parallel}(\vec{b},z)$ is both $\vec{b}$ and z dependent, geometry is eliminated in the latter models by explicit integration over the impact parameter so that only a tube containing N nucleons ($N = 1,2,3,\ldots$) is encountered by the projectile nucleon. The number of nucleons encountered actually increases as the collisions become more central (i.e., small impact parameter ($b \to 0$) collisions). Since an expression like $Q_{\parallel}(\vec{b},z)$ is explicitly density dependent, the present model offers some advantage over the high-energy models such as the SSM.

Further insight can be gained by examining the Glauber model (ref. 28) expression for the average number of nucleons encountered by an incident nucleon as it propagates through a nucleus:

$$T(b,z) \approx \sigma_{NN} \int_{-\infty}^{z} dz' \rho_T\left(\vec{b},z'\right) \tag{8}$$

This is shown in figure 1 for a proton incident on a lead target. We assume $\sigma_{NN} \approx 40$ mb and use a Saxon-Woods density distribution for the lead nucleus with a half-density radius of 6.624 fm and a skin thickness of 1.73 fm. Also shown is the mean number of nucleons (encountered) in the SSM, that
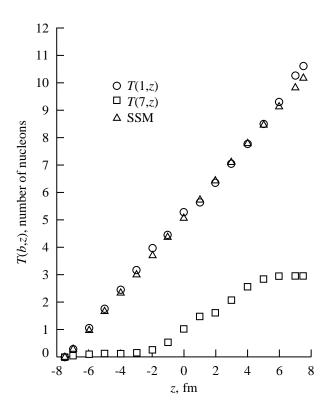
Figure 1. Average number of nucleons encountered by a proton incident on a Pb nucleus as a function of impact parameter b (fm), and depth along beam direction z. Also shown is mean number of nucleons in the SSM.

Figure 2. Momentum loss as a function of depth by an incident high-energy proton on a Pb target for two impact parameters.

is, $\overline{N}(z) = \rho_o \sigma_{NN} z$, with $\rho_o = 0.17$ fm^{-3}, where z is the depth. Note that only for small impact parameter collisions do $T(b,z)$, and $\overline{N}(z)$ agree with each other, as expected.

3. Results

In order to compare the predictions of this model with those from other models, as well as with experimental results, we first focus on proton-nucleus collisions. The momentum loss suffered by an incident proton is plotted in figure 2 for a lead target at various depths z (fm) and at two different impact parameters as the projectile traverses the target (the losses are given in the projectile-nucleus center-of-mass (CM) frame). The results are normalized to the asymptotic values of momentum loss, $Q(b,\infty)$, in each case. The maximum recoil momentum of the incident proton is shown in figure 3(a) as a function of target mass number, the latter ranging between 12 (for carbon) and 238 (for uranium). In figure 3(b), the mean number of inelastic collisions, $\nu = A_T \sigma_{\text{inel}}/\sigma_{\text{reac}}$ is plotted; σ_{inel} and σ_{reac} are the proton-nucleon inelastic cross section and proton-nucleus reaction cross sections, respectively.
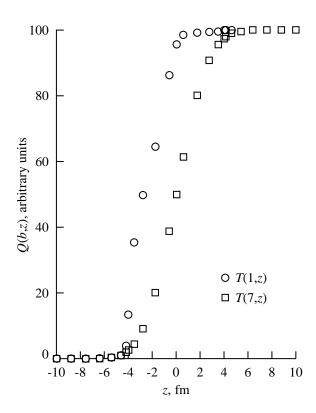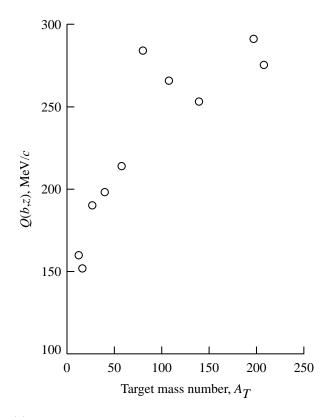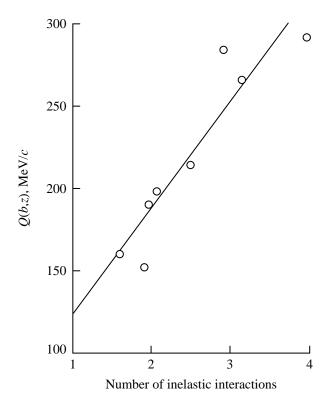
The value of σ_{inel} at high energy is known to be ≈ 32 mb, whereas σ_{reac} is taken from compilations (ref. 29). Only an intermediate impact parameter collision is treated here; the actual magnitude of the impact parameter is target dependent. One perhaps might expect beam momentum loss to scale in a linear way with ν, the number of inelastic collisions the proton undergoes in the target. This is observed in our calculations as can be readily seen in figure 3(b).

The number densities of target nuclei (Woods-Saxon type for $A \geq 20$ and harmonic well for $A < 20$) are taken from compilations (ref. 29). The appropriate equations to convert the quantities for the projectile in its rest system (PRS) into the center of mass (CM) or the laboratory (L) frame quantities and vice versa (CM to PRS, CM to L) are given in the appendix. We are not aware of any set of experiments, other than the ones already cited, that measure recoil momenta in proton-nucleus collisions. This is not so in the heavy ion case, where such studies have a long history (ref. 30). Because of the paucity of data, we have decided to compare our results with other theoretical model predictions of longitudinal momentum transfer in proton-nucleus collisions.

$Q(b,z)$, MeV/c (vertical axis, left plot)

Target mass number, A_T (horizontal axis, left plot)

$Q(b,z)$, MeV/c (vertical axis, right plot)

Number of inelastic interactions (horizontal axis, right plot)

(a) As a function of target mass number for a proton incident on targets ranging from ^{12}C through ^{238}U.

(b) Versus mean number of inelastic collisions.

Figure 3. Maximum recoil momentum of a high-energy proton ($E_P = 1$ GeV).

One such model is the Intranuclear Cascade (INC) model and the code VEGAS (ref. 31). Results for the average forward momentum imparted to the struck nucleus as a function of bombarding energy are plotted in figure 4 for a ^{238}U target (also see fig. 2 of ref. 31). Results are plotted for the INC calculations and from this work. For the INC code, the average recoil momentum increases with bombarding energy for the uranium target. It also increases with the mass number of the target (fig. 2 of ref. 31) in the INC. This is also true in the present work, as can be seen in figures 3(a) and 3(b). The energy dependence of the momentum transfer is similar in the present model, as shown in figure 4. Note that the present model yields a distribution of recoil momenta of the target nucleus as a function of impact parameter, much as the INC does. Our calculation only yields an "average" value and, as currently formulated, is incapable of yielding standard deviations around this mean value. Therefore, when a single value of recoil momentum is quoted, it is understood to be averaged over a range of impact parameters following reference 27, since the INC quotes an "average" value as well. Note that the av-

erage forward momentum imparted to the struck nucleus is only a small fraction of the momentum of the incident proton, and this fraction decreases as incident beam energy decreases. In figure 4 we plot the "average" value of forward (longitudinal) momentum (with and without pion production) obtained with our model. The value without pions ranges from 89 MeV/c at an incident energy of $E_p = 400$ MeV up to ≈ 116 MeV/c at $E_p = 1800$ MeV. From figure 4, the differences between predictions of our model and the INC are typically of the order of ≈ 100 MeV/c or larger. Part of this may be due to the neglect of alpha and other complex fragment emissions in the INC code. Inclusion of these processes in the cascade would lower the average forward momentum imparted to the struck nucleus, thus reducing the differences between cascade predictions and the present work. The momentum "downshifts" (average parallel momentum transfer) associated with pion production are sizeable (refs. 26 and 32). It has been shown (ref. 32), for example, that the longitudinal momentum transfer (or the "downshift") in pion production may range from ≈ 370 MeV/c at threshold to ≈ 100 MeV/c at $E_p = 1$ GeV in the projectile rest
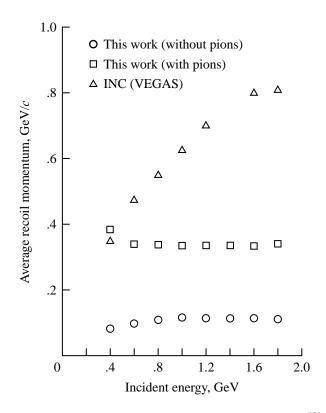
Figure 4. Average forward component of momentum for ^{238}U target and predictions from INC calculations.

Figure 5. Linear recoil momentum from present work and from INC calculations for ^{12}C +^{12} C at $E/A = 800$ MeV.

frame. These values, when converted to the laboratory frame, are of the order of the magnitude of the discrepancy between the cascade predictions and those from this work (fig. 4). Further work is necessary to pin down additional sources of the discrepancy.

For the nucleus-nucleus case, we first compare with the Intranuclear Cascade (INC) code of Yariv and Fraenkel (ref. 33), which is a direct generalization of the VEGAS code (ref. 34). The code treats accurately the multiple collision processes in the nucleus but disregards completely the possible NN correlations (see refs. 33 and 34 for a detailed description). The calculation reproduces the linear recoil momentum distribution of the residual nucleus at the end of the cascade. The results are shown in figure 5 for ^{12}C + ^{12}C at $E/A = 800$ MeV. The histogram corresponds to the total recoil momentum. The differences may arise from the particular choice of physics input in the cascade code, for example, the lack of mean field or they may arise from the different choices for the nuclear densities in the two calculations (harmonic well in the present work). Clearly, more work is needed in order to pinpoint the sources
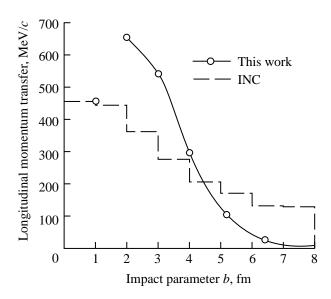
of these differences.

Next, we compare the predictions of the present work with those from the Vlasov-Uehling-Uhlenbeck (VUU) simulations by Aichelin and Stöcker (ref. 35) and Aichelin (ref. 36) on stopping power for $84A$-MeV ^{12}C-induced reactions on targets ranging from ^{12}C through ^{197}Au. At small impact parameters ($b \approx 1$ fm), these authors found that for the ^{12}C target, roughly 60 percent of the center-of-mass momentum was transferred to the midrapidity source, while projectile remnants continued with essentially beam velocity. This midrapidity source subsequently lost 75 percent of its momentum because of NN collisions. For heavier targets, such as ^{58}Ni and ^{197}Au, roughly 66 and 80 percent of the maximum momentum transfer allowed by kinematics for each target was transferred. In addition, the projectile was completely stopped in the target for Ni through Au targets. In figure 6, we compare results from this work with those obtained by Aichelin and Stöcker (ref. 35). The agreement is again reasonably good, especially for the heavier targets.

The detailed impact parameter dependence of longitudinal momentum transfer is compared with the quantum molecular dynamics (QMD) calculations of Aichelin (ref. 36) for ^{12}C + ^{12}C in figure 7 for a bombarding energy $E/A = 84$ MeV. There is reasonable agreement. It can be seen from figure 7 that the present model tends to predict longitudinal

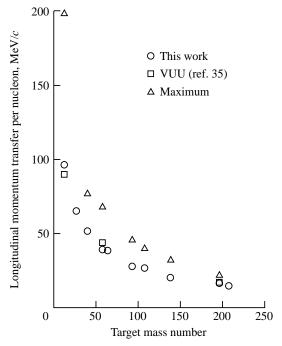momentum transfers that differ by about 10 percent compared with VUU or QMD calculations.

Figure 6. Longitudinal momentum transfer per nucleon to target-like residue as a function of impact parameter b for ^{12}C-induced reactions on targets ranging from ^{12}C through ^{197}Au at $E/A = 85$ MeV. Triangles represent maximum momentum transfer possible from kinematics.
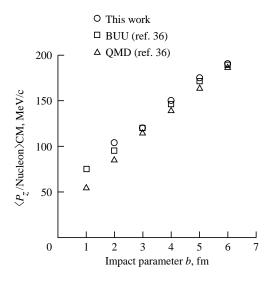

Figure 7. Longitudinal momentum per nucleon, carried by fragments in the reaction ^{12}C $+$ ^{12}C at $E/A = 84$ MeV as a function of impact parameter b (fm). Also shown are results from Aichelin (ref. 36) within BUU and QMD model frameworks.

4. Concluding Remarks

In this work, we attempted to answer the question, "How much of the incident momentum does a nucleon or nucleus lose as it collides with a nuclear target?" This was done within the framework of a description of momentum loss based on multiple scattering theory. Using an experimental nucleon-nucleon (NN) transition matrix and the appropriate nuclear matter densities, we predict longitudinal momentum transfers to projectiles, targets, and their remnants. The beam energies considered range from hundreds of MeV to a few GeV per nucleon. These predictions are both impact parameter dependent and depth dependent. Results for proton stopping power are in reasonable agreement with the data and with predictions from the sequential scattering models. For both proton-nucleus and nucleus-nucleus collisions, our predictions agree reasonably well with those from the Intranuclear Cascade (INC), Vlasov-Uehling-Uhlenbeck (VUU), and quantum molecular dynamics (QMD) model simulations.

The capabilities of the present model are extensive. With only the imaginary part of the NN transition matrix and nuclear number densities as inputs, the present model accurately predicts longitudinal momentum transfer in nuclear collisions. These predictions depend on impact parameter $\vec{b}$, depth z, and energy. It is clear that just as the real part of the NN transition matrix largely determines transverse momentum transfer, the imaginary component predominantly determines momentum loss suffered by the incident projectile on nuclear targets.

NASA Langley Research Center
Hampton, VA 23681-0001
November 3, 1993

Appendix

Coordinate System Transformations

In the rest system of the projectile, the center-of-mass velocity β_{CM} and the Lorentz factor γ_{CM} are given as

$$\left.\begin{array}{l} \beta_{\mathrm{CM}} = \vec{P}_T / \left(E_T + M_P \right) \\[2mm] \gamma_{\mathrm{CM}} = 1/\sqrt{1 - \beta_{\mathrm{CM}}^2} \end{array}\right\} \qquad (\mathrm{A1})$$

where M_P is the total mass of the projectile and $\vec{P}_T$ and E_T are the three momenta and energy of the target.

In the present work, we calculate longitudinal momentum transfer in the projectile-target center-of-mass (CM) system. Let $\langle Q_z \rangle$, P_z, and P_z' be the average longitudinal momentum transfer, and the initial and final momenta of the projectile in its rest system (PRS), such that

$$\langle Q_z \rangle = P_z - P_z' = -P_z' \qquad (\mathrm{A2})$$

since $P_z = 0$ by definition in this frame; $\langle Q_z \rangle$ indicates an average value, since $Q_z(b)$ is an impact parameter dependent quantity, and we approximate it at *one* impact parameter b. The appropriate transformation from the center-of-mass frame (barred quantities) is then

$$\overline{P}_z = \gamma_{\mathrm{CM}} \left(P_z - \beta_{\mathrm{CM}} M_P \right) = -\gamma_{\mathrm{CM}} \beta_{\mathrm{CM}} M_P \qquad (\mathrm{A3})$$

$$\overline{P}_z' = \gamma_{\mathrm{CM}} \left(P_z' - \beta_{\mathrm{CM}} E_P' \right) = \gamma_{\mathrm{CM}} \left(- \langle Q_z \rangle - \beta_{\mathrm{CM}} E_P' \right)$$

where E_P' is the total energy of the projectile *after* the interaction in its rest system. A reasonable Ansatz for the latter is

$$E_P' = M_P + Q_\perp^2 / 2 M_P \qquad (\mathrm{A4})$$

with $Q_\perp$ the transverse momentum transfer due to the interaction, which is also a function of impact parameter.

References

1. Jeukenne, J. P.; Lejeune, A.; and Mahaux, C.: Many-Body Theory of Nuclear Matter. *Phys. Rep.*, vol. 25, no. 2, 1976, pp. 83–174.

2. Negele, J. W.; and Yazaki, K.: Mean Free Path in a Nucleus. *Phys. Review Lett.*, vol. 47, no. 2, July 13, 1981, pp. 71–74.

3. Fantoni, S.; Friman, B. L.; and Pandharipande, V. R.: The Imaginary Part of the Nucleon Optical Potential in Nuclear Matter. *Phys. Lett.*, vol. 104B, no. 2, Aug. 20, 1981, pp. 89–91.

4. Schiffer, J. P.: Pion Reaction Modes on Nuclei. *Nucl. Phys.*, vol. A335, 1980, pp. 339–352.

5. Nadasen, A.; Schwandt, P.; Singh, P. P.; Jacobs, W. W.; Bacher, A. D.; Debevec, P. T.; Kaitchuck, M. D.; and Meek, J. T.: Elastic Scattering of 80–180 MeV Protons and the Proton-Nucleus Optical Potential. *Phys. Review C*, vol. 23, no. 3, Mar. 1981, pp. 1023–1043.

6. Bohr, Aage; and Mottelson, Ben R.: *Nuclear Structure. Volume I—Single-Particle Motion.* W. A. Benjamin, Inc., 1969.

7. Sobel, Michael I.; Siemens, Philip J.; Bondorf, Jakob P.; and Bethe, H. A.: Shock Waves in Colliding Nuclei. *Nucl. Phys.*, vol. A251, 1975, pp. 502–529.

8. Amsden, Anthony A.; Goldhaber, Alfred S.; Harlow, Francis H.; and Nix, J. Rayford: Relativistic Two-Fluid Model of Nucleus-Nucleus Collisions. *Phys. Review C*, vol. 17, no. 6, June 1978, pp. 2080–2096.

9. Anishetty, R.; Koehler, P.; and McLerran, L.: Central Collisions Between Heavy Nuclei at Extremely High Energies: The Fragmentation Region. *Phys. Review D*, vol. 22, no. 11, Dec. 1, 1980, pp. 2793–2804.

10. Busza, Wit; and Goldhaber, Alfred S.: Nuclear Stopping Power. *Phys. Lett.*, vol. 139B, no. 4, May 17, 1984, pp. 235–238.

11. Foà, L.: Inclusive Study of High-Energy Multiparticle Production and Two-Body Correlations. *Phys. Rep.*, vol. 22, no. 1, 1975, pp. 1–56.

12. Barton, D. S.; Brandenburg, G. W.; Busza, W.; Dobrowolski, T.; Friedman, J. I.; Halliwell, C.; Kendall, H. W.; Lyons, T.; Nelson, B.; Rosenson, L.; Verdier, R.; Chiaradia, M. T.; DeMarzo, C.; Favuzzi, C.; Germinario, G.; Guerriero, L.; LaVopa, P.; Maggi, G.; Posa, F.; Selvaggi, G.; Spinelli, P.; Waldner, F.; Cutts, D.; Dulude, R. S.; Hughlock, B. W.; Lanou, R. E., Jr.; Massimo, J. T.; Brenner, A. E.; Carey, D. C.; Elias, J. E.; Garbincius, P. H.; Polychronakos, V. A.; Nassalski, J.; and Siemiarczuk, T.: Experimental Study of the A Dependence of Inclusive Hadron Fragmentation. *Phys. Review D*, vol. 27, no. 11, June 1, 1983, pp. 2580–2599.

13. Csernai, L. P.; and Kapusta, J. I.: Proton Stopping Power of Heavy Nuclei. *Phys. Review D*, vol. 29, no. 11, June 1, 1984, pp. 2664–2665.

14. Hwa, Rudolph C.: Degradation of Proton Momentum Through Nuclei. *Phys. Review Lett.*, vol. 52, no. 7, Feb. 13, 1984, pp. 492–495.

15. Hüfner, J.; and Klar, A.: Nuclear Stopping Power for Ultrarelativistic Protons. *Phys. Lett.*, vol. 145B, no. 3, 4, Sept. 20, 1984, pp. 167–170.

16. Wong, Cheuk-Yin: Baryon Distribution in Relativistic Heavy-Ion Collisions. *Phys. Review Lett.*, vol. 52, no. 16, Apr. 16, 1984, pp. 1393–1396.

17. Csernai, L. P.; and Kapusta, J. I.: Deceleration of High-Energy Protons by Heavy Nuclei. *Phys. Review D*, vol. 31, no. 11, June 1, 1985, pp. 2795–2799.

18. Lindstrom, P. J.; Greiner, D. E.; Heckman, H. H.; Cork, Bruce, and Bieser, F. S.: *Isotope Production Cross Sections From the Fragmentation of ^{16}O and ^{12}C at Relativistic Energies.* LBL-3650, Lawrence Berkeley Lab., Univ. of California, June 1975.

19. Greiner, D. E.; Lindstrom, P. J.; Heckman, H. H.; Cork, Bruce; and Bieser, F. S.: Momentum Distributions of Isotopes Produced by Fragmentation of Relativistic ^{12}C and ^{16}O Projectiles. *Phys. Review Lett.*, vol. 35, no. 3, July 21, 1975, pp. 152–155.

20. Gerbier, G.; Guoxiao, Ren; and Price, P. B.: Abnormally Large Momentum Loss in Charge Pickup by 900-MeV/Nucleon Au Nuclei. *Phys. Review Lett.*, vol. 60, no. 22, May 30, 1988, pp. 2258–2261.

21. Binns, W. R.; Cummings, J. R.; Garrard, T. L.; Israel, M. H.; Klarmann, J.; Stone, E. C.; and Waddington, C. J.: Charge, Mass, and Energy Changes During Fragmentation of Relativistic Nuclei. *Phys. Review C*, vol. 39, no. 5, May 1989, pp. 1785–1798.

22. Tull, C. E.: *Relativistic Heavy Ion Fragmentation at HISS.* LBL-29718 (Contract No. DE-AC03-76SF00098), Lawrence Berkeley Lab., Univ. of California, Oct. 1990.

23. Budiansky, M. P.; Ahlen, S. P.; Tarle, G.; and Price, P. B.: Study of High-Energy Gamma Rays From Relativistic Nucleus-Nucleus Collisions. *Phys. Review Lett.*, vol. 49, no. 6, Aug. 9, 1982, pp. 361–364.

24. Jacob, M.; and Van, J. Tran Thanh, eds. (with contributions by M. Faessler, J. Kapusta, L. McLerran, J. Rafelski, H. Satz, and W. Willis): Quark Matter Formation and Heavy Ion Collisions. *Phys. Rep.*, vol. 88, no. 5, 1982, pp. 325–329.

25. Khan, F.; Khandelwal, G. S.; Townsend, L. W.; Wilson, J. W.; and Norbury, J. W.: Optical Model Description of Momentum Transfer in Relativistic Heavy Ion Collisions. *Phys. Review C*, third ser., vol. 43, Mar. 1991, pp. 1372–1377.

26. Townsend, L. W.; Wilson, J. W.; Khan, F.; and Khandelwal, G. S.: Momentum Transfer in Relativistic Heavy Ion Charge-Exchange Reactions. *Phys. Review C*, third ser., vol. 44, no. 1, July 1991, pp. 540–542.

27. Khan, F.; Townsend, L. W.; Tripathi, R. K.; and Cucinotta, F. A.: Universal Characteristics of Transverse Momentum Transfer in Intermediate Energy Heavy Ion

Collisions. *Phys. Review C*, vol. 48, no. 2, Aug. 1993, pp. 926–928.

28. Glauber, R. J.: High-Energy Collision Theory. *Lectures in Theoretical Physics, Volume I*, Wesley E. Brittin and Lita G. Dunham, eds., Interscience Publ., Inc., 1959, pp. 315–414.

29. Townsend, Lawrence W.; and Wilson, John W: *Tables of Nuclear Cross Sections for Galactic Cosmic Rays—Absorption Cross Sections.* NASA RP-1134, 1985.

30. Porile, Norbert T.: Momentum Imparted to Complex Nuclei in High-Energy Interactions. *Phys. Review*, vol. 120, no. 2, Oct. 15, 1960, pp. 572–581.

31. Metropolis, N.; Bivins, R.; Storm, M.; Turkevich, Anthony; Miller, J. M.; and Friedlander, G.: Monte Carlo Calculations on Intranuclear Cascades. I. Low-Energy Studies. *Phys. Review*, second ser., vol. 110, no. 1, Apr. 1, 1958, pp. 185–203.

32. Deutchman, P. A.; Maung, K. M.; Norbury, J. W.; Rasmussen, J. O.; and Townsend, L. W.: Δ Excita-tions and Shell-Model Information in Heavy-Ion, Charge-Exchange Reactions. *Phys. Review C*, vol. 34, no. 6, Dec. 1986, pp. 2377–2379.

33. Yariv, Y.; and Fraenkel, Z.: Intranuclear Cascade Calculation of High-Energy Heavy-Ion Interactions. *Phys. Review C*, vol. 20, no. 6, Dec. 1979, pp. 2227–2243.

34. Chen, K.; Fraenkel, Z.; Friedlander, G.; Grover, J. R.; Miller, J. M.; and Shimamoto, Y.: VEGAS: A Monte Carlo Simulation of Intranuclear Cascades. *Phys. Review*, vol. 166, no. 4, Feb. 20, 1968, pp. 949–967.

35. Aichelin, Jörg; and Stöcker, Horst: Longitudinal Momentum Transfer and the Nucleon's Mean Free Path in Medium Energy Heavy Ion Collisions—TDHF Versus Vlasov-Uehling-Uhlenbeck Theory. *Phys. Lett.*, vol. 163B, no. 1, 2, 3, 4, Nov. 21, 1985, pp. 59–65.

36. Aichelin, Jörg: "Quantum" Molecular Dynamics—A Dynamical Microscopic n-Body Approach To Investigate Fragment Formation and the Nuclear Equation of State in Heavy Ion Collisions. *Phys. Rep.*, vol. 202, no. 5 & 6, 1991, pp. 233-361.

REPORT DOCUMENTATION PAGE

1. AGENCY USE ONLY *(Leave blank)*	2. REPORT DATE December 1993	3. REPORT TYPE AND DATES COVERED Technical Paper

4. TITLE AND SUBTITLE
Momentum Loss in Proton-Nucleus and Nucleus-Nucleus Collisions

5. FUNDING NUMBERS
WU 199-45-16-11

6. AUTHOR(S)
Ferdous Khan and Lawrence W. Townsend

7. PERFORMING ORGANIZATION NAME(S) AND ADDRESS(ES)
NASA Langley Research Center
Hampton, VA 23681-0001

8. PERFORMING ORGANIZATION REPORT NUMBER
L-17304

9. SPONSORING/MONITORING AGENCY NAME(S) AND ADDRESS(ES)
National Aeronautics and Space Administration
Washington, DC 20546-0001

10. SPONSORING/MONITORING AGENCY REPORT NUMBER
NASA TP-3405

11. SUPPLEMENTARY NOTES
Khan: Old Dominion University, Norfolk, VA; Townsend: Langley Research Center, Hampton, VA.

12a. DISTRIBUTION/AVAILABILITY STATEMENT

Unclassified–Unlimited

Subject Category 73

12b. DISTRIBUTION CODE

13. ABSTRACT *(Maximum 200 words)*
An optical model description, based on multiple scattering theory, of longitudinal momentum loss in proton-nucleus and nucleus-nucleus collisions is presented. The crucial role of the imaginary component of the nucleon-nucleon transition matrix in accounting for longitudinal momentum transfer is demonstrated. Results obtained with this model are compared with Intranuclear Cascade (INC) calculations, as well as with predictions from Vlasov-Uehling-Uhlenbeck (VUU) and quantum molecular dynamics (QMD) simulations. Comparisons are also made with experimental data where available. These indicate that the present model is adequate to account for longitudinal momentum transfer in both proton-nucleus and nucleus-nucleus collisions over a wide range of energies.

14. SUBJECT TERMS
Nuclear collisions; Momentum loss; Proton-nucleus reactions; Nucleus-nucleus reactions

15. NUMBER OF PAGES
11

16. PRICE CODE
A03

17. SECURITY CLASSIFICATION OF REPORT Unclassified	18. SECURITY CLASSIFICATION OF THIS PAGE Unclassified	19. SECURITY CLASSIFICATION OF ABSTRACT	20. LIMITATION OF ABSTRACT